Dufour and Radiation absorption effects on unsteady MHD free convection Casson fluid flow past an exponentially infinite vertical plate through porous medium.

S. Rama Mohan[1*], Prof. G. Viswanatha Reddy[2], Prof.S.V.K.Varma[2]
[1,2,] Department of Mathematics, S.V.University, Tirupathi-517502,A.P,India.

Abstract: The aim of the present paper is to study the effects of Dufour and Radiation absorption on an unsteady MHD free convection Casson fluid flow past an exponentially an infinite vertical plate through porous medium in the presence of thermal radiation and heat source or sink. Chemical reaction is assumed in the first order. The set of non-dimensional partial differential equations are solved analytically by using the Laplace transform technique. The influence of various non-dimensional parameters on the velocity, the temperature, the concentration, the skin friction, the local Nusselt and the Sherwood numbers are discussed and derived through graphs and tables. The velocity profile decreases with increases the values of Magnetic parameter, Radiation absorption, chemical reaction and thermal radiation. The temperature profile increases with an increase the values of thermal radiation and Dufour number.

Keywords: Casson fluid, Dufour, Radiation absorption, MHD, thermal radiation and chemical reaction.

Introduction

The study of non-Newtonian fluid through porous medium has number of applications in science and Engineering. The number of investigators has investigated in non-Newtonian fluid like Casson fluid which exhibits the yield stress. In the human body the blood also can be treated as Casson fluid. Casson fluid model is widely used in food stuffs and biological materials, especially blood. It describes the steady shear stress and shear rate behavior of blood. The number of investigators has investigated their pioneer work done by Casson [1] analyzed a flow equation for pigment oil suspensions of the printing ink type. The application of the minimal energy hypothesis to a Casson fluid was studied by Mcgregor [2]. A mathematical study of peristaltic transport of a Casson fluid was found by Mermone et al. [3]. Raptis and Perdikis [4] examined unsteady flow through a highly porous medium in the presence of radiation. Boyd et al. [5] discussed analysis of the Casson and Carreau-Yasuda non-Newtonian blood models in steady and oscillatory flows using the lattice boltzmann method. Unsteady boundary layer flow of a Casson fluid due to an impulsively started moving flat plate was discussed by Mustafa et al. [6]. Raptis [7] analyzed free convective oscillatory flow and mass transfer past a porous plate in the presence of radiation for an optically thin fluid. Soret and Dufour effects on the magneto hydrodynamic (MHD) flow of the Casson fluid over a stretched surface were discussed by Hayath et al. [8]. Nadeem et al. [9] investigated MHD flow of a Casson fluid over an exponentially shrinking sheet. Effects of mass transfer on MHD flow of Casson fluid with chemical reaction was analyzed by Shehzad et al. [10]. Bhattacharyya [11] studied boundary layer stagnation-point flow of Casson fluid and heat transfer towards a shrinking/stretching sheet. Bhattacharyya [12] found MHD stagnation-point flow of Casson fluid and heat transfer over a stretching sheet with thermal radiation. Mukhopadhyay and Vajravelu [13] presented diffusion of chemically reactive species in Casson fluid flow over an unsteady permeable stretching surface. Subba Rao et al. [14] considered heat transfer in a Casson rheological fluid from a semi-infinite vertical plate with partial slip. Mukhopadhyay et al. [15] investigated Casson fluid flow over an unsteady stretching surface. Shehzad et al. [16] identified effects of mass transfer on MHD flow of Casson fluid with chemical reaction and suction. Sarojanamm et al. [17] examined MHD Casson fluid flow, heat and mass transfer in a vertical channel with stretching Walls. Casson fluid flow and heat transfer past an exponentially porous stretching surface in presence of thermal radiation discussed by Pramanik [18]. Animasaun [19] analyzed effects of thermophoresis, variable viscosity and thermal conductivity on free convective heat and mass transfer of non-darcian MHD dissipative Casson fluid flow with suction and nth order of chemical reaction. Unsteady boundary layer flow and heat transfer of a Casson fluid past an oscillating vertical plate with Newtonian heating was explored by Hussanan et al. [20]. Makanda et al. [21] presented diffusion of chemically reactive species in Casson fluid flow over an unsteady stretching surface in porous medium in the presence of a magnetic field. MHD mixed convection flow of a Casson fluid over an exponentially stretching surface with the effects of Soret and Dufour, thermal radiation and chemical reaction was found by Sharada and Shankar [22]. Saqib et al. [23] considered heat and mass transfer phenomena in the flow of Casson fluid over an infinite oscillating plate in the presence of first-order chemical reaction and slip effect. Reddy [24] studied unsteady radiative convective boundary layer flow of a Casson fluid with variable thermal conductivity. Casson fluid flow and heat transfer over an unsteady porous stretching surface was studied by Kirubhashankar et al. [25]. Ahmed et al. [26] explored effects on magnetic field in squeezing flow of a Casson fluid between parallel plates. Kumar and Gangadhar [27] researched effect of chemical reaction on slip flow of MHD Casson fluid over a stretching sheet with heat and mass transfer. Newtonian heating effect on steady hydro magnetic Casson fluid flow a plate with heat and mass transfer was discussed by Das et al. [28]. MHD boundary layer heat and mass transfer of a chemically reacting Casson fluid over a permeable stretching surface with non-uniform heat source/sink was examined by Gireesha et al. [29]. Sarma and Pandit [30] analyzed effects of hall current rotation and Soret effects on MHD free convection heat and mass transfer flow past an accelerated vertical plate through a porous medium. Raju et al. [31] considered heat and mass transfer in magneto hydrodynamic Casson fluid over an exponentially permeable stretching surface. Kataria and Patel [32] presented Soret and heat generation effects on MHD Casson fluid flow past an oscillating vertical plate embedded through porous medium. Unsteady squeezing flow of Casson fluid with magneto hydrodynamic effect and passing through porous medium was discussed by Khan et al. [33]. Reddy et al. [34] studied radiation absorption and chemical reaction effect on MHD flow of heat generating Casson fluid past oscillating vertical porous plate. Heat and mass transfer in unsteady MHD Casson fluid flow with convective boundary conditions was investigated by Puspalatha et al. [35]. Uallah et al. [36] examined Unsteady MHD mixed convection slip flow of Casson fluid over nonlinearly stretching sheet embedded in a porous medium with chemical reaction, thermal radiation, heat generation/absorption and convective boundary conditions. Mohan et al. [37] discussed thermal radiation and chemical reaction effects on unsteady MHD free convection flow of a viscous dissipative Casson fluid past an exponentially accelerated infinite vertical plate through porous medium with TGHS. Veeresh et al. [38] investigated the Joule heating and thermal diffusion effect on MHD radiative and convective Casson fluid flow past an oscillating semi-infinite vertical porous plate.

In the present study, we analyzed the effects of Dufour, Radiation absorption, thermal radiation, chemical reaction and heat source or sink on flow of Casson fluid past an exponentially infinite vertical plate through porous medium. The set of partial differential equations are solved analytically by using Laplace Transform technique. The influence of various non-dimensional quantities on the velocity, the temperature, the concentration, the skin friction, and the local Nusselt and the Sherwood numbers are thoroughly investigated and presented through graphs and tables.

Mathematical formulation

Consider an un steady MHD free convection heat and mass transfer flow of a viscous, incompressible, electrically, conducting, radiating and chemically reacting fluid past an exponentially accelerated infinite vertical plate. A uniform magnetic field B_0 applied in a transverse direction to the fluid flow. Let x^*-axis is taken along the plate in vertical upward direction to the fluid flow and y^*-axis is taken normal to it in the direction of applied transverse magnetic field. Initially, when$t^* \leq 0$, both the fluid and plate are at stationary condition having constant temperature and concentration. When t^*>0, the plate is exponentially accelerated with the velocity $u^* = u_0\, e^{a^* t^*}$ .At the same time, the plate the temperature is raised linearly with time t and also the concentration is raised to C_w^*. A uniform magnetic fieldB_0 is applied in to y-direction. For free convection flow, it is also taken that, the induced magnetic field is assumed to be negligible as the magnetic Reynolds number of the flow is taken to be very small. The viscous dissipation is not considered in to the energy equation. The influences of variation in density (ρ) with temperature and species concentration are considered only on the body force term, in accordance with usual Boussinesq approximations. The fluid assumed here is gray, absorbing/emitting radiation but a non-scattering medium. Since the flow of the fluid is taken to be in the direction of x^*-axis, so the physical quantities are functions of the space co-ordinate $y^*$and t^*only. The rheological equation of state for an isotropic and incompressible flow of a Casson fluid is as follows

$$\tau_{ij} = \begin{cases} 2\left(\mu_\alpha + \frac{P_y}{\sqrt{2\pi}}\right) e_{ij}, & \pi > \pi_c \\ 2\left(\mu_\alpha + \frac{P_y}{\sqrt{2\pi}}\right) e_{ij}, & \pi < \pi_c \end{cases}$$

Here $\pi = e_{ij} e_{ij}$ and e_{ij} are the $(i,j)^{th}$ component of the deformation rate,

π -the product of the component of the deformation rate with itself,

π_c-a critical value of this product based on the non-Newtonian model,

π_α-plastic dynamic viscosity of non-Newtonian fluid and

P_y- The yield stress of the fluid.

The governing equations as follows

Momentum Equation:

$$\frac{\partial u^*}{\partial t^*} = v\left(1+\frac{1}{\beta}\right)\frac{\partial^2 u^*}{\partial y^{*2}} + g\beta_T^*(T^* - T_\infty^*) + g\beta_C^*(C^* - C_\infty^*) - \frac{\sigma B_0^2}{\rho}u^* - \frac{v}{K}u^* \tag{1}$$

Energy Equation:

$$\frac{\partial T^*}{\partial t^*} = \frac{\kappa}{\rho C_P}\frac{\partial^2 T^*}{\partial y^{*2}} - \frac{1}{\rho C_P}\frac{\partial q_r}{\partial y^*} + \frac{D_m K_T}{C_S C_P}\frac{\partial^2 C^*}{\partial y^{*2}} - \frac{Q^*}{\rho C_P}(T^* - T_\infty^*) + \frac{Q_1}{\rho C_P}(C^* - C_\infty^*) \tag{2}$$

Diffusion Equation:

$$\frac{\partial C^*}{\partial t^*} = D_m \frac{\partial^2 C^*}{\partial y^{*2}} - Kr(C^* - C_\infty^*) \tag{3}$$

The initial and boundary conditions are:

$$\begin{aligned} & t^* \le 0, u^* = 0, T^* = T_\infty^*, C^* = C_\infty^* \ \text{for all } y^* \\ & t^* > 0,\ u^* = u_0 e^{a^* t^*}, T^* = T_\infty^* + (T_W^* - T_\infty^*)t^*, C^* = C_W^* \ \text{at } y^* = 0 \\ & \qquad u^* \to 0, T^* \to T_\infty^*, C^* \to C_\infty^* \ \text{as } y \to \infty \end{aligned} \tag{4}$$

Where $u^* \beta, \beta_T^*, \beta_C^*, B_0, v, \kappa, \rho, T^*, C^*, C_p, C_s, q_r, Q, \sigma, D_m, t, a, Du, D_1$, Sc, K, Pr $and\ K_r$

are respectively Casson parameter, the fluid velocity in the x^*- direction, coefficient of thermal expansion, coefficient of expansion with concentration, external magnetic field, kinematic viscosity, thermal conductivity, fluid density, temperature of the fluid, Species concentration, Specific heat at constant pressure, Concentration susceptibility, radiative heat flux, heat absorption, electric conductivity, Coefficient of mass diffusivity, time, acceleration parameter, Dufour number, Radiation absorption, Schmidt number, porosity parameter, Prandtl number and chemical reaction parameter.

The radiative heat flux q_r, under Rosseland approximation of the form

$$q_r = -\frac{4\sigma^*}{3k^*}\frac{\partial T^*}{\partial y^*} \tag{5}$$

Here σ*-the Stefan-Boltzmann constant and

k^*- The mean absorption coefficient.

It assumed that the temperature differences within the flow are sufficiently small and that T^{*4} may be expressed as a linear combination of the temperature. This can be found by expanding T^{*4} in a Taylor series about T_∞^* and neglecting the higher order terms, thus we get

$$T^{*4} = 4T_\infty^{*3}T^* - 3T_\infty^{*4}. \tag{6}$$

From Eq.5. and Eq. 6, then Eq.2. reduces to

$$\frac{\partial T^*}{\partial t^*} = \frac{\kappa}{\rho C_P}\frac{\partial^2 T^*}{\partial y^{*2}} - \frac{16\sigma^* T_\infty^*}{3\rho C_p k^*}\frac{\partial^2 T^*}{\partial y^{*2}} + \frac{D_m K_T}{C_S C_P}\frac{\partial^2 C^*}{\partial y^{*2}} - \frac{Q^*}{\rho C_P}(T^* - T_\infty^*) + \frac{Q_1}{\rho C_P}(C^* - C_\infty^*) \tag{7}$$

On introducing the given non- dimensional quantities are

$$u = \frac{u^*}{u_0}, y = \frac{u_0}{v}y^*, t = \frac{u_0^2}{v}t^*, K = \frac{k^* u_0^2}{v}, M = \frac{\sigma B_0^2 v}{\rho u_0^2}, \theta = \frac{(T^* - T_\infty^*)}{(T_w^* - T_\infty^*)}, \phi = \frac{(C^* - C_\infty^*)}{(C_w^* - C_\infty^*)},$$
$$Sc = \frac{v}{D}, Du = \frac{D_m K_T}{T_m v(T_w^* - T_\infty^*)}, Gr = \frac{vg\beta_T(T_w^* - T_\infty^*)}{u_0^3}, Gm = \frac{vg\beta_C^*(C_w^* - C_\infty^*)}{u_0^3},$$
$$\Pr = \frac{\rho v C_p}{\kappa}, k = \frac{k^* u_0^2}{v}, Q = \frac{Q^* v}{\rho C_p u_0^2}, R = \frac{16\sigma^* T_\infty^*}{3k^* k}, Q_1 = \frac{Q^* v(C^* - C_\infty^*)}{\rho C_p u_0^2 (T_w^* - T_\infty^*)}, a = \frac{v}{u_0^2}a^* \tag{8}$$

In view of Eq.8.then Eq.1, Eq.3, Eq.7, reduce to the following non-dimensional forms

$$\frac{\partial u}{\partial t} = \left(1 + \frac{1}{\alpha}\right)\frac{\partial^2 u}{\partial y^2} - \left(M + \frac{1}{K}\right)u + Gr\,\theta + Gm\,\phi \tag{9}$$

$$\frac{\partial \theta}{\partial t} = \left(\frac{1+R}{\Pr}\right)\frac{\partial^2 \theta}{\partial y^2} + Du\frac{\partial^2 \phi}{\partial y^2} - Q\theta + Q_1\phi \tag{10}$$

$$\frac{\partial \phi}{\partial t} = \frac{1}{Sc}\frac{\partial^2 \phi}{\partial y^2} - Kr\,\phi \tag{11}$$

The corresponding boundary conditions reduces to

$$t \le 0,\ u = 0, \theta = 0, \phi = 0\ for\ all\ y,$$
$$t > 0, u = e^{at}, \theta = t, \phi = 1 at\ y = 0,$$
$$u \to 0, \theta \to 0, \phi \to 0\ as\ y \to \infty. \qquad (12)$$

Solution of the Problem:

The system of Eq.9. Eq.10 and Eq.11.with subject to the boundary conditions in Eq.12, are solved by analytically using Laplace Transform technique and the expressions for

$$\phi(y,t) = \frac{1}{2}\left[\exp\left(-y\sqrt{Sc\,kr}\right) erfc\left(\frac{y\sqrt{Sc}}{2\sqrt{t}} - \sqrt{Kr\,t}\right) + \exp\left(y\sqrt{Sc\,kr}\right) erfc\left(\frac{y\sqrt{Sc}}{2\sqrt{t}} + \sqrt{Kr\,t}\right)\right] \qquad (13)$$

$$\theta(y,t) = \left[B_1 + \left[b\left[1 + \frac{Kr}{c}\right] + \frac{d}{c}\right]B_3 - \left[\frac{b\,Kr}{c} + \frac{d}{c}\right]B_2 - \left[b\left[1 + \frac{Kr}{c}\right] + \frac{d}{c}\right]B_4 - \left[\frac{b\,Kr}{c} + \frac{d}{c}\right]B_5\right] \qquad (14)$$

$$u(y,t) = B_6 - \frac{f}{g}B_7 - \left[\begin{matrix}\frac{f}{g^2} \\ -\left[\frac{b\,Kr}{c} + \frac{d}{c}\right]\left[\frac{f}{g} - \frac{m}{n}\right] + \frac{e}{n}\end{matrix}\right]B_8 + \left[\frac{f}{g^2} + \left[\begin{matrix} b\left[1 + \frac{Kr}{c}\right] \\ + \frac{d}{c}\end{matrix}\right]\left[\frac{f}{c-g} - \frac{m}{c-n}\right]\right]B_9$$
$$-\left[\left[b\left[1 + \frac{Kr}{c}\right] + \frac{d}{c}\right]\frac{f}{c-g} + \left[\frac{b\,Kr}{c} + \frac{d}{c}\right]\frac{f}{g}\right]B_{10} + \left[\begin{matrix}\left[b\left[1 + \frac{Kr}{c}\right] + \frac{d}{c}\right]\frac{m}{c-n} \\ + \left[\frac{b\,Kr}{c} + \frac{d}{c}\right]\frac{m}{n} + \frac{e}{n}\end{matrix}\right]B_{11} + \frac{f}{g}B_1$$
$$+\left[\begin{matrix}\frac{f}{g^2} \\ -\left[\frac{b\,Kr}{c} + \frac{d}{c}\right]\frac{f}{g}\end{matrix}\right]B_2 - \left[\begin{matrix}\frac{f}{g^2} + \\ \left[b\left[1 + \frac{Kr}{c}\right] + \frac{d}{c}\right]\frac{f}{c-g}\end{matrix}\right]B_3 + \left[\begin{matrix}\left[b\left[1 + \frac{Kr}{c}\right] + \frac{d}{c}\right]\frac{f}{c-g} \\ + \left[\frac{b\,Kr}{c} + \frac{d}{c}\right]\frac{f}{g}\end{matrix}\right]B_{12}$$
$$+\left[\left[b\left[1 + \frac{Kr}{c}\right] + \frac{d}{c}\right]\frac{m}{c-n}\right]B_4 + \left[\left[\frac{b\,Kr}{c} + \frac{d}{c}\right]\frac{m}{n} + \frac{e}{n}\right]B_5 - \left[\begin{matrix}\left[b\left[1 + \frac{Kr}{c}\right] + \frac{d}{c}\right]\frac{m}{c-n} \\ + \left[\frac{b\,Kr}{c} + \frac{d}{c}\right]\frac{m}{n} + \frac{e}{n}\end{matrix}\right]B_{13} \qquad (15)$$

Here

$$B_1=\left[\left(\frac{t}{2}-\frac{y\sqrt{A_1}}{4\sqrt{Q}}\right)\exp\left(-y\sqrt{A_1Q}\right)erfc\left(\frac{y\sqrt{A_1}}{2\sqrt{t}}-\sqrt{Qt}\right)+\left(\frac{t}{2}+\frac{y\sqrt{A_1}}{4\sqrt{Q}}\right)\exp\left(y\sqrt{A_1Q}\right)erfc\left(\frac{y\sqrt{A_1}}{2\sqrt{t}}+\sqrt{Qt}\right)\right]$$

$$B_2=\frac{1}{2}\left[\exp\left(-y\sqrt{A_1Q}\right)erfc\left(\frac{y\sqrt{A_1}}{2\sqrt{t}}-\sqrt{Qt}\right)+\exp\left(y\sqrt{A_1Q}\right)erfc\left(\frac{y\sqrt{A_1}}{2\sqrt{t}}+\sqrt{Qt}\right)\right]$$

$$B_3=\frac{e^{ct}}{2}\left[\exp\left(-y\sqrt{A_1(c+Q)}\right)erfc\left(\frac{y\sqrt{A_1}}{2\sqrt{t}}-\sqrt{(c+Q)t}\right)+\exp\left(y\sqrt{A_1(c+Q)}\right)erfc\left(\frac{y\sqrt{A_1}}{2\sqrt{t}}+\sqrt{(c+Q)t}\right)\right]$$

$$B_4=\frac{e^{ct}}{2}\left[\exp\left(-y\sqrt{Sc(c+kr)}\right)erfc\left(\frac{y\sqrt{Sc}}{2\sqrt{t}}-\sqrt{(c+Kr)t}\right)+\exp\left(y\sqrt{Sc(c+kr)}\right)erfc\left(\frac{y\sqrt{Sc}}{2\sqrt{t}}+\sqrt{(c+Kr)t}\right)\right]$$

$$B_5=\frac{1}{2}\left[\exp\left(-y\sqrt{Sc\,kr}\right)erfc\left(\frac{y\sqrt{Sc}}{2\sqrt{t}}-\sqrt{Kr\,t}\right)+\exp\left(y\sqrt{Sc\,kr}\right)erfc\left(\frac{y\sqrt{Sc}}{2\sqrt{t}}+\sqrt{Kr\,t}\right)\right]$$

$$B_6=\frac{e^{at}}{2}\left[\exp\left(-y\sqrt{A_5(a+A_6)}\right)erfc\left(\frac{y\sqrt{A_5}}{2\sqrt{t}}-\sqrt{(a+A_6)t}\right)+\exp\left(y\sqrt{A_5(a+A_6)}\right)erfc\left(\frac{y\sqrt{A_5}}{2\sqrt{t}}+\sqrt{(a+A_6)t}\right)\right]$$

$$B_7=\left[\left(\frac{t}{2}-\frac{y\sqrt{A_5}}{4\sqrt{A_6}}\right)\exp\left(-y\sqrt{A_5A_6}\right)erfc\left(\frac{y\sqrt{A_5}}{2\sqrt{t}}-\sqrt{A_6t}\right)+\left(\frac{t}{2}+\frac{y\sqrt{A_5}}{4\sqrt{A_6}}\right)\exp\left(y\sqrt{A_5A_6}\right)erfc\left(\frac{y\sqrt{A_5}}{2\sqrt{t}}+\sqrt{A_6t}\right)\right]$$

$$B_8=\frac{1}{2}\left[\exp\left(-y\sqrt{A_5A_6}\right)erfc\left(\frac{y\sqrt{A_5}}{2\sqrt{t}}-\sqrt{A_6t}\right)+\exp\left(y\sqrt{A_5A_6}\right)erfc\left(\frac{y\sqrt{A_5}}{2\sqrt{t}}+\sqrt{A_6t}\right)\right]$$

$$B_9=\frac{e^{ct}}{2}\left[\exp\left(-y\sqrt{A_5(c+A_6)}\right)erfc\left(\frac{y\sqrt{A_5}}{2\sqrt{t}}-\sqrt{(c+A_6)t}\right)+\exp\left(y\sqrt{A_5(c+A_6)}\right)erfc\left(\frac{y\sqrt{A_5}}{2\sqrt{t}}+\sqrt{(c+A_6)t}\right)\right]$$

$$B_{10}=\frac{e^{gt}}{2}\left[\exp\left(-y\sqrt{A_5(g+A_6)}\right)erfc\left(\frac{y\sqrt{A_5}}{2\sqrt{t}}-\sqrt{(g+A_6)t}\right)+\exp\left(y\sqrt{A_5(g+A_6)}\right)erfc\left(\frac{y\sqrt{A_5}}{2\sqrt{t}}+\sqrt{(g+A_6)t}\right)\right]$$

$$B_{11}=\frac{e^{nt}}{2}\left[\exp\left(-y\sqrt{A_5(n+A_6)}\right)erfc\left(\frac{y\sqrt{A_5}}{2\sqrt{t}}-\sqrt{(n+A_6)t}\right)+\exp\left(y\sqrt{A_5(n+A_6)}\right)erfc\left(\frac{y\sqrt{A_5}}{2\sqrt{t}}+\sqrt{(n+A_6)t}\right)\right]$$

$$B_{12}=\frac{e^{nt}}{2}\left[\exp\left(-y\sqrt{A_1(n+Q)}\right)erfc\left(\frac{y\sqrt{A_1}}{2\sqrt{t}}-\sqrt{(n+Q)t}\right)+\exp\left(y\sqrt{A_1(n+Q)}\right)erfc\left(\frac{y\sqrt{A_1}}{2\sqrt{t}}+\sqrt{(n+Q)t}\right)\right]$$

$$B_{13}=\frac{e^{nt}}{2}\left[\exp\left(-y\sqrt{Sc(n+kr)}\right)erfc\left(\frac{y\sqrt{Sc}}{2\sqrt{t}}-\sqrt{(n+Kr)t}\right)+\exp\left(y\sqrt{Sc(n+kr)}\right)erfc\left(\frac{y\sqrt{Sc}}{2\sqrt{t}}+\sqrt{(n+Kr)t}\right)\right]$$

Where

$$A_1=\frac{\Pr}{1+R},A_2=A_1Du,A_3=A_1Q_1,A_4=1+\frac{1}{\beta},A_5=\frac{1}{A_3},A_6=M+\frac{1}{K},b=\frac{Sc\,A_2}{Sc-A_1},c=\frac{A_1Q-Sc\,Kr}{Sc-A_1},$$

$$d=\frac{A_3}{Sc-A_1},e=\frac{Gm\,A_5}{Sc-A_5},f=\frac{GrA_5}{A_1-A_5},g=\frac{A_5A_6-A_1Q}{A_1-A_5},m=\frac{GrA_5}{Sc-A_5},n=\frac{A_5A_6-ScKr}{Sc-A_5}.$$

Sherwood Number: The rate of change of mass transfer is given by

$$Sh=-\left[\frac{\partial\phi}{\partial y}\right]_{y=0} \tag{16}$$

From Eq.13. and Eq.16, we get the Sherwood number is given below

$$Sh=\left[\sqrt{ScKr}\,erf\left(\sqrt{Kr\,t}\right)+\sqrt{\frac{Sc}{\pi t}}e^{-Kr\,t}\right]$$

Nussle number: The rate of change of heat transfer is given by

$$Nu=-\left[\frac{\partial\theta}{\partial y}\right]_{y=0} \tag{17}$$

From Eq.14 and Eq.17, we get Nussle number is given below

$$Nu=\left[D_1+\left[b\left[1+\frac{Kr}{c}\right]+\frac{d}{c}\right]D_3-\left[\frac{bKr}{c}+\frac{d}{c}\right]D_2-\left[b\left[1+\frac{Kr}{c}\right]+\frac{d}{c}\right]D_4-\left[\frac{bKr}{c}+\frac{d}{c}\right]D_5\right]$$

Skin friction coefficient: The rate of change of velocity is given by

$$\tau=-\left(1+\frac{1}{\alpha}\right)\left[\frac{\partial u}{\partial y}\right]_{y=0} \tag{18}$$

From Eq.15 and Eq.18, we get Skin friction is given below

$$\tau=\left(1+\frac{1}{\alpha}\right)\left[D_6-\frac{f}{g}D_7-\left[\frac{f}{g^2}-\left[\frac{b\,Kr}{c}+\frac{d}{c}\right]\left[\frac{f}{g}-\frac{m}{n}\right]+\frac{e}{n}\right]D_8+\left[\begin{array}{l}\frac{f}{g^2}+\\ \left[b\left[1+\frac{Kr}{c}\right]+\frac{d}{c}\right]\left[\frac{f}{c-g}-\frac{m}{c-n}\right]\end{array}\right]D_9\right.$$

$$-\left[\left[b\left[1+\frac{Kr}{c}\right]+\frac{d}{c}\right]\frac{f}{c-g}+\left[\frac{b\,Kr}{c}+\frac{d}{c}\right]\frac{f}{g}\right]D_{10}+\left[\left[b\left[1+\frac{Kr}{c}\right]+\frac{d}{c}\right]\frac{m}{c-n}+\left[\frac{b\,Kr}{c}+\frac{d}{c}\right]\frac{m}{n}+\frac{e}{n}\right]D_{11}$$

$$+\frac{f}{g}D_1+\left[\frac{f}{g^2}-\left[\frac{b\,Kr}{c}+\frac{d}{c}\right]\frac{f}{g}\right]D_2-\left[\begin{array}{l}\frac{f}{g^2}+\\ \left[b\left[1+\frac{Kr}{c}\right]+\frac{d}{c}\right]\frac{f}{c-g}\end{array}\right]D_3+\left[\begin{array}{l}\left[b\left[1+\frac{Kr}{c}\right]+\frac{d}{c}\right]\frac{f}{c-g}\\ +\left[\frac{b\,Kr}{c}+\frac{d}{c}\right]\frac{f}{g}\end{array}\right]D_{12}$$

$$\left.+\left[\left[b\left[1+\frac{Kr}{c}\right]+\frac{d}{c}\right]\frac{m}{c-n}\right]D_4+\left[\left[\frac{b\,Kr}{c}+\frac{d}{c}\right]\frac{m}{n}+\frac{e}{n}\right]D_5-\left[\begin{array}{l}\left[b\left[1+\frac{Kr}{c}\right]+\frac{d}{c}\right]\frac{m}{c-n}\\ +\left[\frac{b\,Kr}{c}+\frac{d}{c}\right]\frac{m}{n}+\frac{e}{n}\end{array}\right]D_{13}\right]$$

Here

$$D_1=\frac{1}{2}\sqrt{\frac{A_1}{Q}}erf\left(\sqrt{Qt}\right)+t\sqrt{A_1Q}\,erf\left(\sqrt{Qt}\right)+\sqrt{\frac{tA_1}{\pi}}e^{-Qt}$$

$$D_2=\sqrt{A_1Q}erf\left(\sqrt{Qt}\right)+\sqrt{\frac{A_1}{\pi t}}e^{-Qt}$$

$$D_3=e^{ct}\left[\sqrt{A_1(c+Q)}erf\left(\sqrt{(c+Q)t}\right)+\sqrt{\frac{A_1}{\pi t}}e^{-(c+Q)t}\right]\;D_4=e^{ct}\left[\sqrt{Sc(c+Kr)}\,erf\left(\sqrt{(c+Kr)t}\right)+\sqrt{\frac{Sc}{\pi t}}e^{-(c+Kr)t}\right]$$

$$D_5=\sqrt{ScKr}erf\left(\sqrt{Kr\,t}\right)+\sqrt{\frac{Sc}{\pi t}}e^{-Kr\,t}$$

$$D_6=e^{at}\left[\sqrt{A_5(a+A_6)}erf\left(\sqrt{(a+A_6)t}\right)+\sqrt{\frac{A_5}{\pi t}}e^{-(a+A_6)t}\right]$$

$$D_7=\frac{1}{2}\sqrt{\frac{A_5}{A_6}}erf\left(\sqrt{A_6\,t}\right)+t\sqrt{A_5A_6}erf\left(\sqrt{A_6\,t}\right)+\sqrt{\frac{tA_5}{\pi}}e^{-A_6t}$$

$$D_8=\left[\sqrt{A_5A_6}erf\left(\sqrt{A_6\,t}\right)+\sqrt{\frac{A_5}{\pi t}}e^{-A_6t}\right]$$

$$D_9=e^{ct}\left[\sqrt{A_5(c+A_6)}erf\left(\sqrt{(c+A_6)t}\right)+\sqrt{\frac{A_5}{\pi t}}e^{-(c+A_6)t}\right]\;D_{10}=e^{gt}\left[\sqrt{A_5(g+A_6)}erf\left(\sqrt{(g+A_6)t}\right)+\sqrt{\frac{A_5}{\pi t}}e^{-(g+A_6)t}\right]$$

$$D_{11}=e^{nt}\left[\sqrt{A_5(n+A_6)}erf\left(\sqrt{(n+A_6)t}\right)+\sqrt{\frac{A_5}{\pi t}}e^{-(n+A_6)t}\right]\;D_{12}=e^{gt}\left[\sqrt{A_1(g+Q)}erf\left(\sqrt{(g+Q)t}\right)+\sqrt{\frac{A_1}{\pi t}}e^{-(g+Q)t}\right]$$

$$D_{13}=e^{nt}\left[\sqrt{Sc(n+Kr)}\,erf\left(\sqrt{(n+Kr)t}\right)+\sqrt{\frac{Sc}{\pi t}}e^{-(n+Kr)t}\right]$$

Where

$$A_1=\frac{\Pr}{1+R},A_2=A_1Du,A_3=A_1Q_1,A_4=1+\frac{1}{\beta},A_5=\frac{1}{A_3},A_6=M+\frac{1}{K},$$

$$b=\frac{Sc\,A_2}{Sc-A_1},c=\frac{A_1Q-Sc\,Kr}{Sc-A_1},d=\frac{A_3}{Sc-A_1},e=\frac{Gm\,A_5}{Sc-A_5},f=\frac{GrA_5}{A_1-A_5},$$

$$g=\frac{A_5A_6-A_1Q}{A_1-A_5},m=\frac{GrA_5}{Sc-A_5},n=\frac{A_5A_6-ScKr}{Sc-A_5}.$$

erfc = Complementary Error function

erf = Error function

Results and Discussion:

The systems of linear non-dimensional equations (9)-(11), with the help of corresponding boundary conditions are solved analytically by using the Laplace Transform technique. The obtained solution reveals that the flow, heat and mass transfer of the fluid will be effected by various non-dimensional governing parameters, such as Casson parameter (α), Magnetic parameter (*M*), Permeability parameter (*K*), Prandtl number *(Pr)*, thermal Grashof number (*Gr*), mass Grashof number (*Gm*), thermal Radiation parameter (*R*), Dufour number *(Du)*, heat absorption parameter (*Q*), Radiation absorption parameter *(Q1)*, acceleration parameter (*a*), Schmidt number (*Sc*), chemical reaction parameter (*Kr*) and time *(t)*. Hence the distribution of velocity, temperature and concentration are studied by the graphs which are obtained by Matlab package. Also the numerical values of skin friction, Nusselt number and Sherwood number are presented in tables. Figures (1) to (23) are drawn to discuss the case of cooling ($Gr>0$, $Gm>0$) and heating ($Gr<0$, $Gm<0$) of the plate. The heating and cooling takes place by setting up free convection currents due to temperature and concentration gradient.

The influence of Magnetic parameter *(M)* and Prandtl number *(Pr)* on the fluid velocity are shown in figures (1) and (2), respectively for the cases cooling and heating of the plate. It is observed that the fluid velocity decreases as *M or Pr* increases in case of cooling of the plate and opposite phenomenon is observed in case of heating of the plate. Velocity decreases with increasing Magnetic parameter due to the fact that applied transverse magnetic field produces a drag in the form of Lorentz force thereby decreasing the magnitude of velocity. Also increase in Pr leads to an enhancement in the viscosity of the fluid or decrease in the thermal diffusivity of the fluid, this will result a gradual reduction in the flow of velocity of the fluid.

Figure (3), shows that the effect of porosity parameter *(K)* on velocity distribution in case of cooling and heating of the plate. It is found that velocity decreases as *K* increases in case of cooling of the plate. But a reverse effect is identified in case of heating of plate. Figure (4), depicts the effects of thermal Grashof number *(Gr)*, mass Grashof number *(Gm))* on velocity distribution in cases cooling and heating of the plate. From this we observed that the velocity increases as *Gr or Gm* increases in case of cooling of the plate and a reverse effects is noticed in case of heating of the plate.

The effects of heat absorption parameter *(Q)* and thermal radiation *(R)* on velocity distribution are shown figures (5) and (6), in cases cooling and heating of the plate. It is seen that velocity decreases as *Q or R* increases in case of cooling of the plate and opposite phenomenon is observed in case of heating of the plate. Therefore using radiation we can control the flow characteristic and temperature distribution.

Figures (7) and (8**),** exhibits the effects of Schmidt number *(Sc)* and chemical reaction *(Kr)* on velocity distribution in case of cooling and heating of the plate. It is found that velocity decreases as *Sc or Kr* increases in case of cooling of the plate. But the result is quite opposite in case of heating of plate.

Figure (9), depicts the behavior of Dufour number *(Du)* on velocity distribution in case of cooling and heating of the plate. It is found that velocity increases as *Du* increases in case of cooling of the plate. But a reverse effect is identified in case of heating of plate. The influence of Radiation absorption parameter *(Q1)* on velocity distribution is shown figure (10), in case of cooling and heating of the plate. We observe that velocity decreases as *Q1* decreases in case of cooling of the plate. But a reverse effect is identified in case of heating of plate. The effect of Casson parameter *(β)* on velocity distribution is shown figure (11), in case cooling and heating of the plate. It is observed that velocity increases as β increases in case of cooling of the plate and it is noticed opposite phenomenon in case of heating of the plate. The influence of time (t) on velocity distribution is shown figure **(12),** in case cooling and heating of the plate. From this it is seen that velocity increases as time *(t)* increases in case of cooling and reverse phenomenon is observed in case of heating of the plate. Figure **(13),** shows the effect of acceleration parameter *(a)* on velocity distribution in case of cooling and heating of the plate. It is found that velocity increases as acceleration parameter *(a)* increases in case of cooling of the plate. But a same effect is identified in case of heating of plate. When a=0 we get the uniform velocity.

The effect of Prandtl number *(Pr)* on the fluid temperature is shown in figure **(14).** It is observed that temperature increases initially and slowly reduces as *Pr* increases of the fluid flow. Because, Prandtl number *(Pr)* is the ratio of kinematic viscosity to thermal diffusivity. The effect of heat source parameter *(Q)* on the fluid temperature is shown in figure **(15).** It is observed that temperature decreases as *Q* increases on the fluid flow. Also, the positive sign of *Q* indicates the heat generation (heat source) whereas negative means heat absorption (heat sink). Heat source physically implies generation of heat from the surface (this is due to $T_w > T_\infty$), which increases temperature in the flow field. Therefore, as heat source parameter increased, temperature increases steeply and exponentially from the surface. The influence of heat source parameter $Q > 0$ on temperature distribution is very much significantly related to the heat sink parameter $Q < 0$. These results are clearly supported from the physical point of view.

The effect of thermal radiation *(R)* on the fluid temperature is shown in figure **(16).** From this it is seen that temperature decreases initially and slowly reduces as *R* increases of the fluid flow.

The effects of Dufour number *(Du)* and Radiation absorption parameter *(Q1)* on the fluid temperature are shown in figures **(17) to (18).** It is observed that temperature increases as *Du or Q1* increases on the fluid flow. The influences of the Schmidt number *(Sc)* and chemical reaction *(Kr)* on the fluid temperature are shown in figure **(19) and (20).**It is clear that temperature increases initially and slowly reduces as *Sc or Kr* increases of the fluid flow. The influence of time *(t)* on temperature distribution is shown in figure **(21).** It is noticed that temperature increases as *t* increases on the fluid flow.

The effects of Schmidt number *(Sc)* and chemical reaction *(Kr)* on concentration distribution in figures **(22) and (23).** It is observed that concentration distribution decreases as *Sc or Kr* increases on the fluid flow. This is due to the fact that chemical reaction in this system results in consumption of the chemical and hence results in decrease of concentration distribution. The most important effect is that the first order chemical reaction has a tendency to diminish the overshoot in the profiles of the solute concentration in the solute boundary layer.

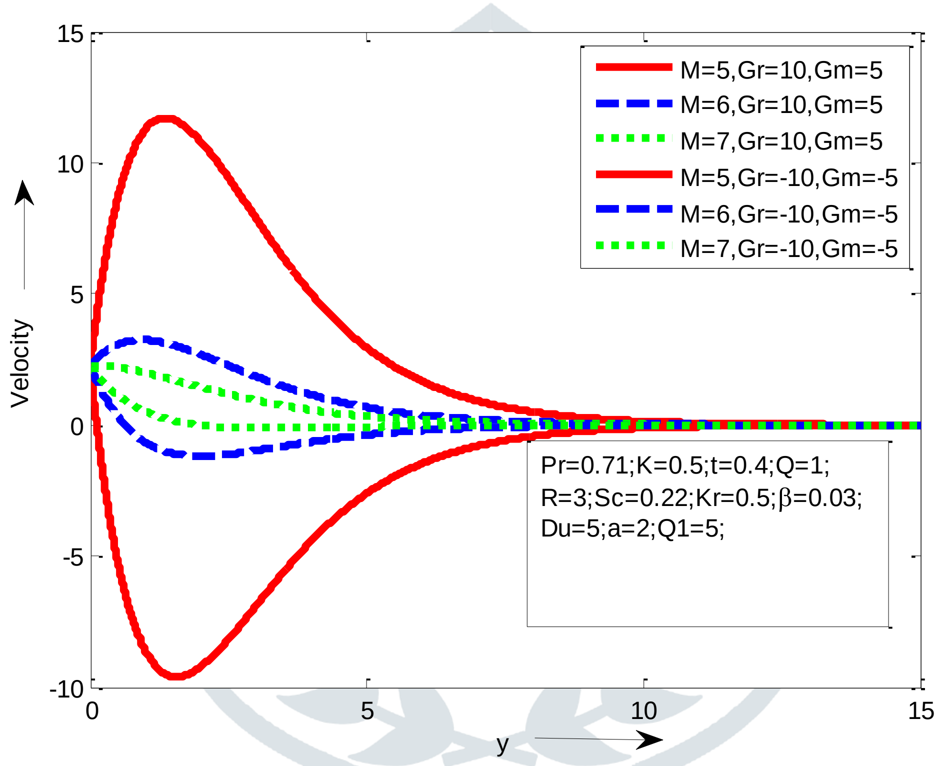

Figure1. The influence of *M* on Velocity.

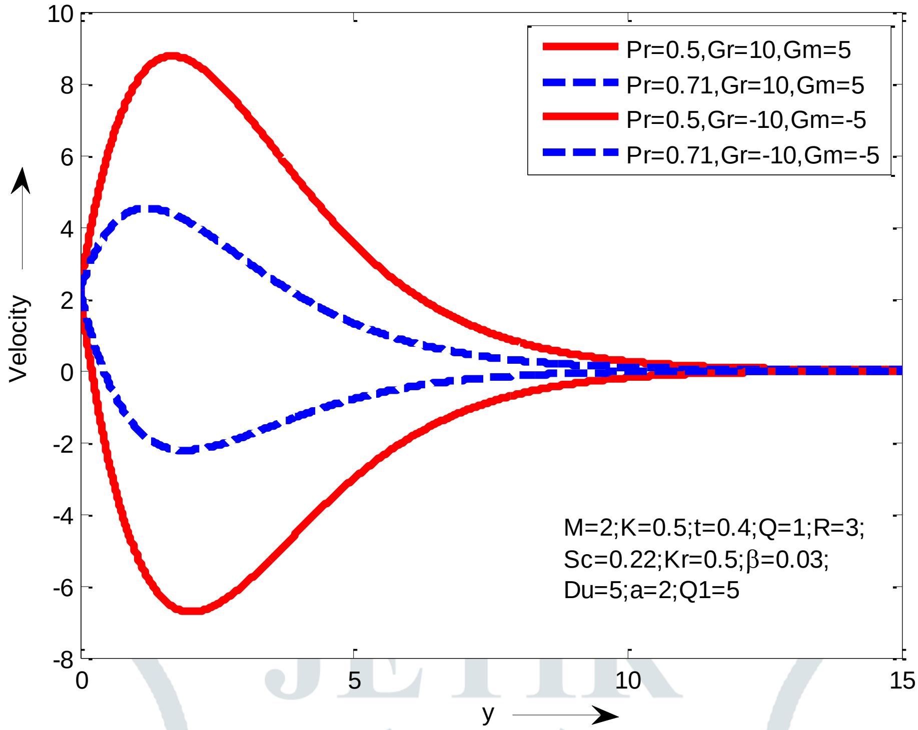

Figure 2. The influence of *Pr* on Velocity.

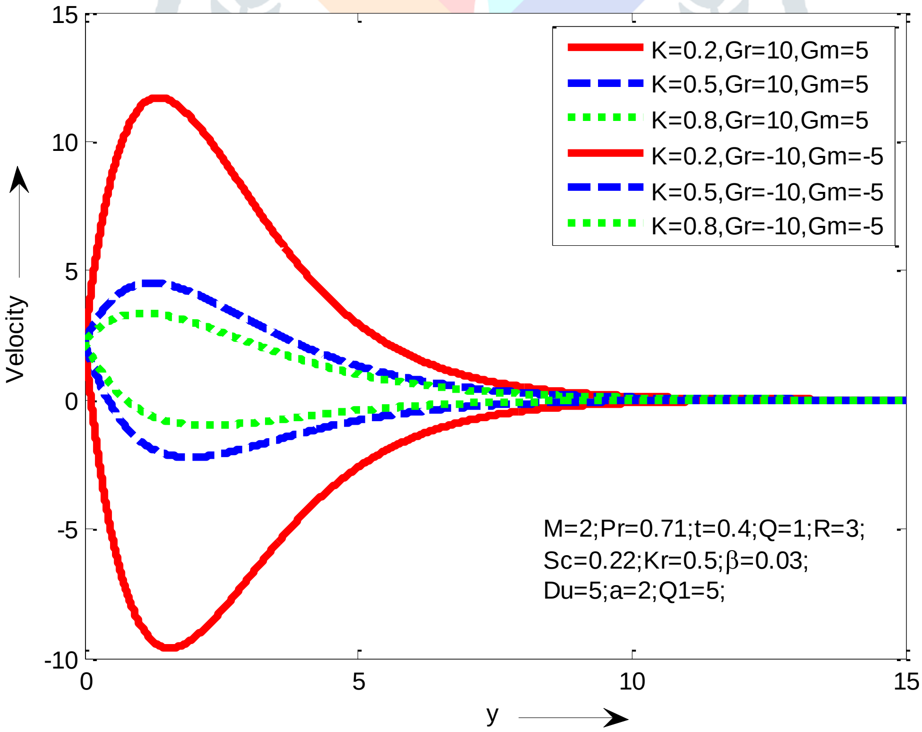

Figure 3. The influence of *K* on Velocity.

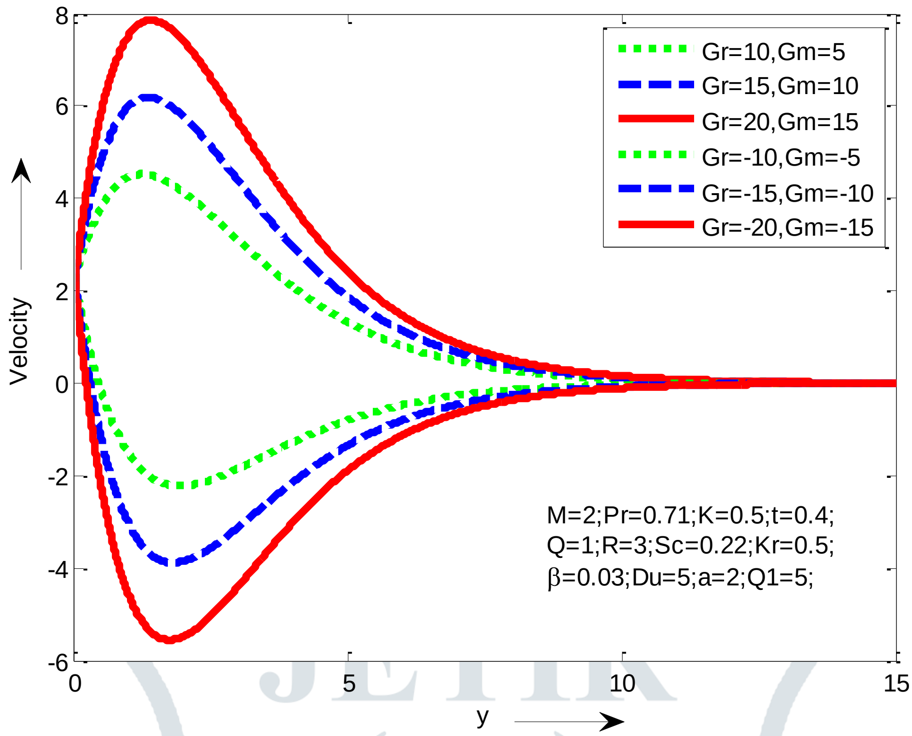

Figure 4. The influence of *Gr* ,*Gm* on Velocity.

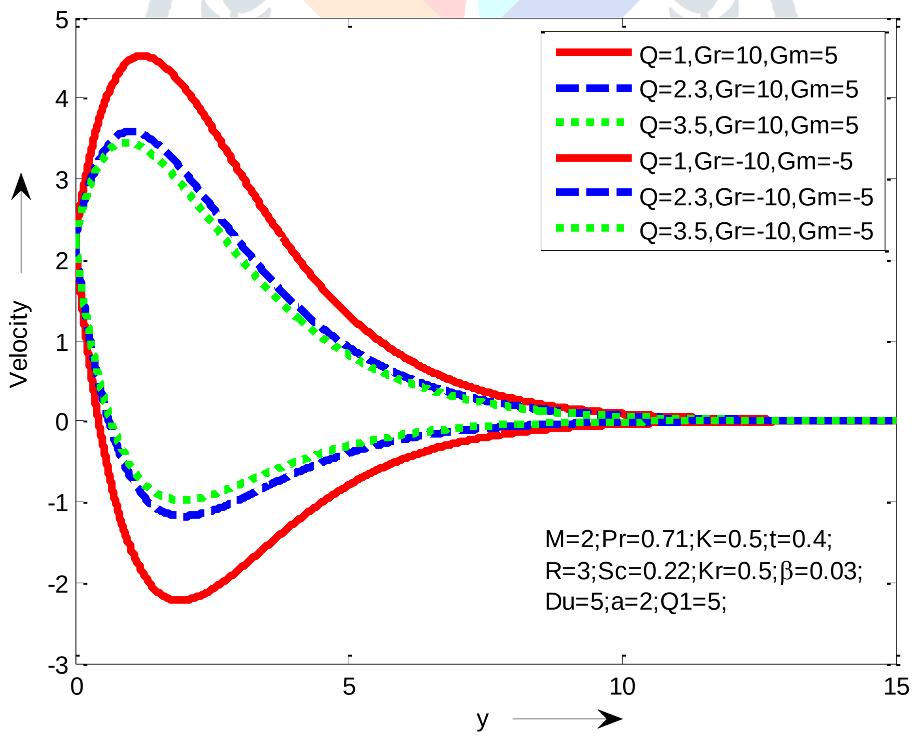

Figure 5. The influence of *Q* on Velocity.

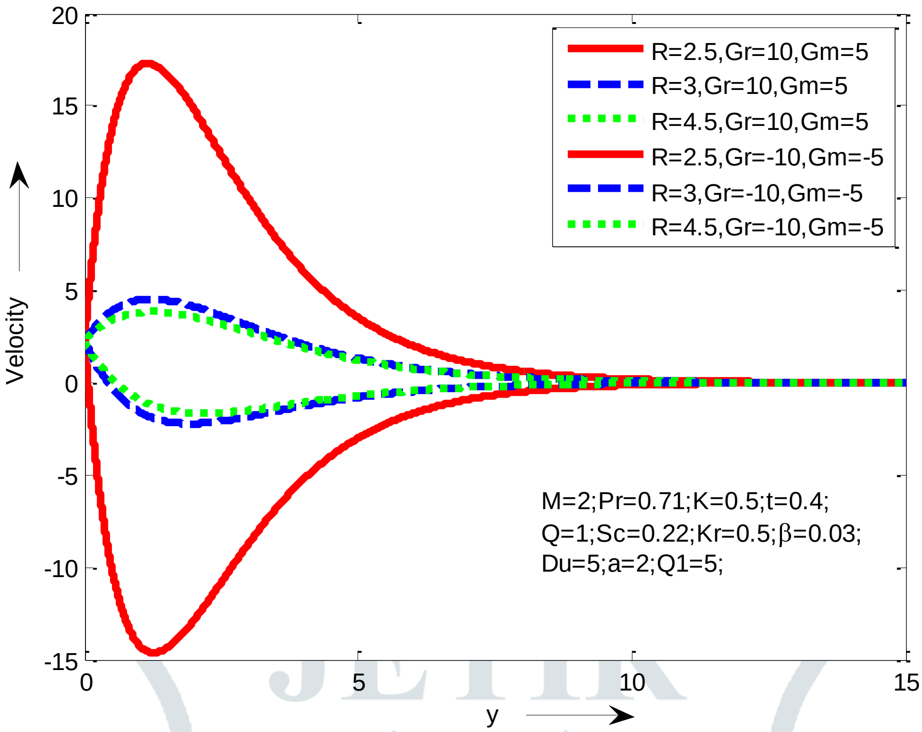

Figure 6. The influence of *R* on Velocity.

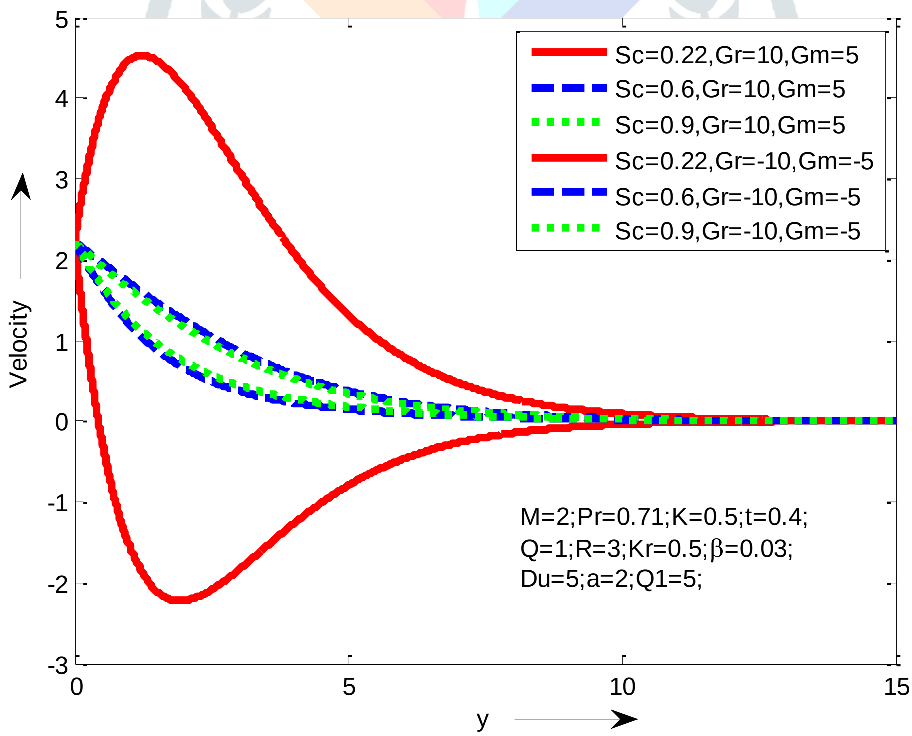

Figure 7. The influence of *Sc* on Velocity.

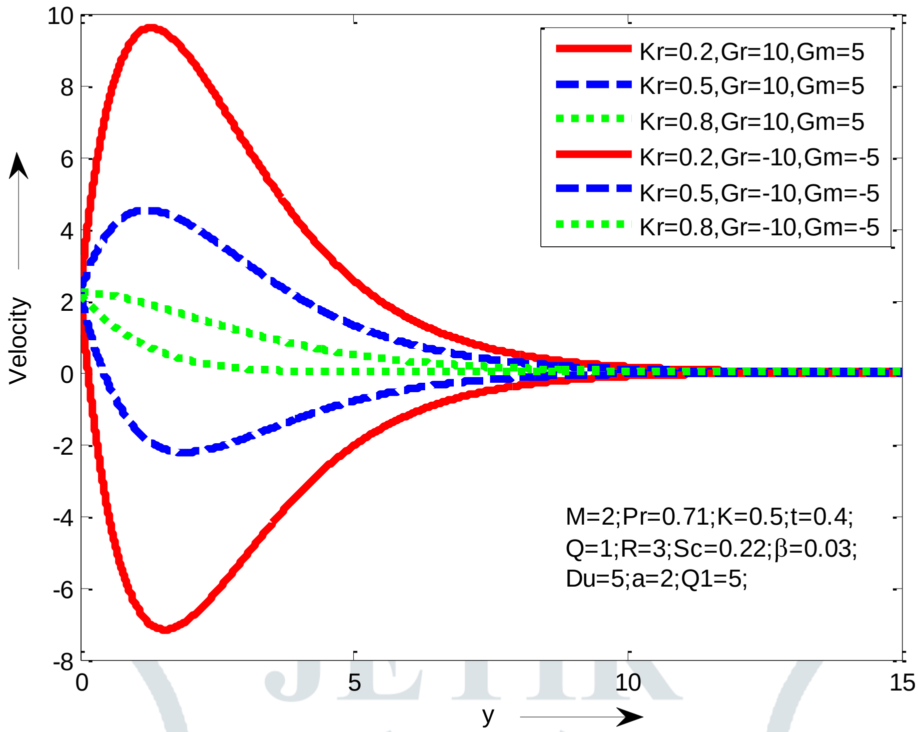

Figure 8. The influence of *Kr* on Velocity.

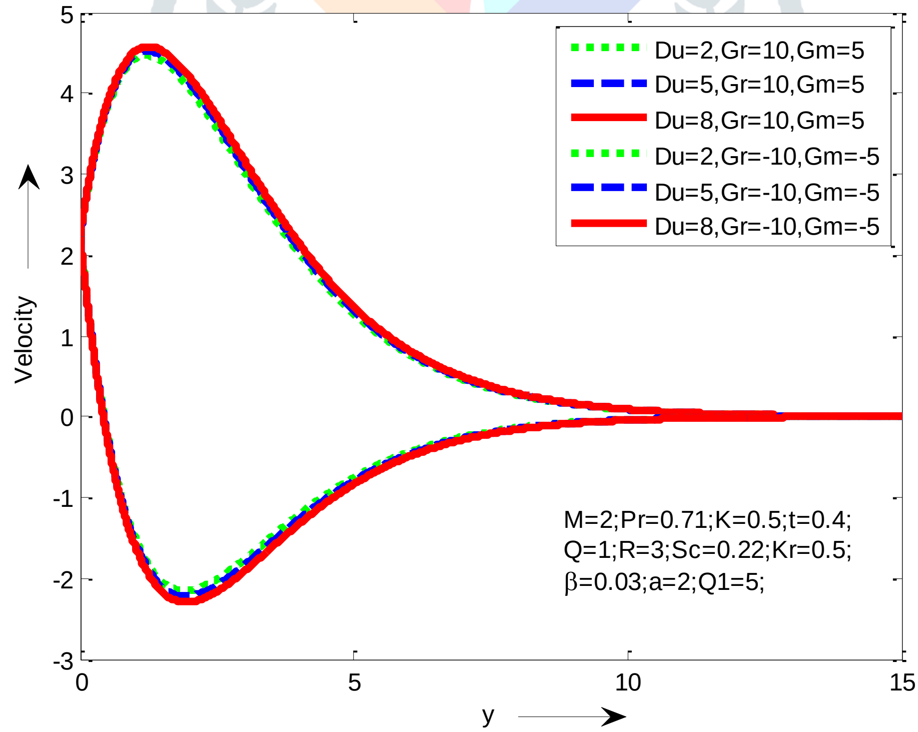

Figure 9. The influence of *Du* on Velocity.

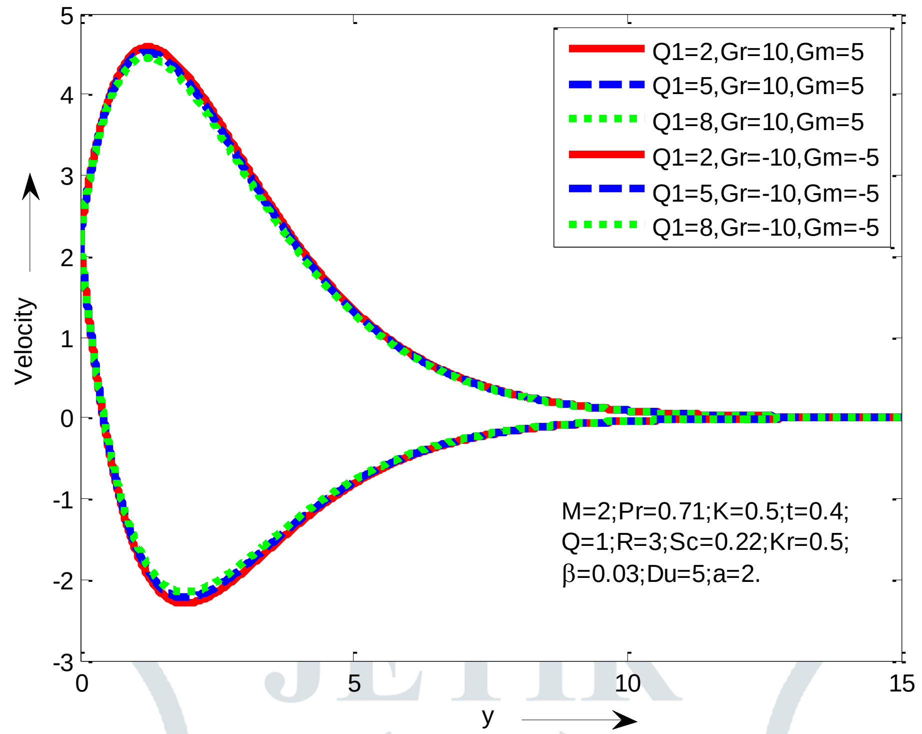

Figure 10. The influence of *Q1* on Velocity.

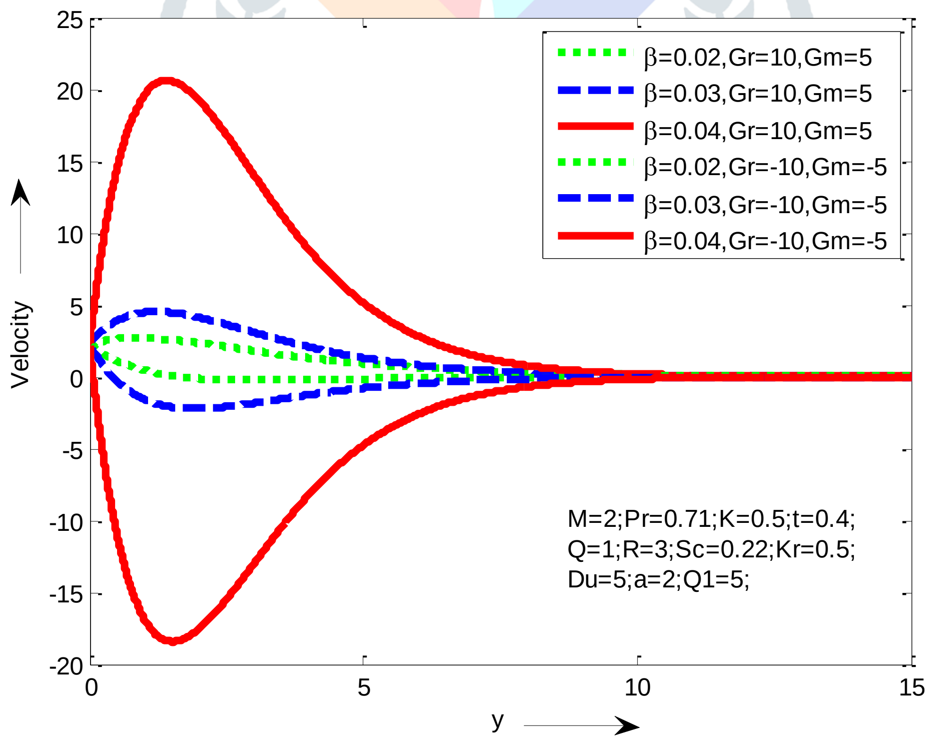

Figure 11. The influence of β on Velocity.

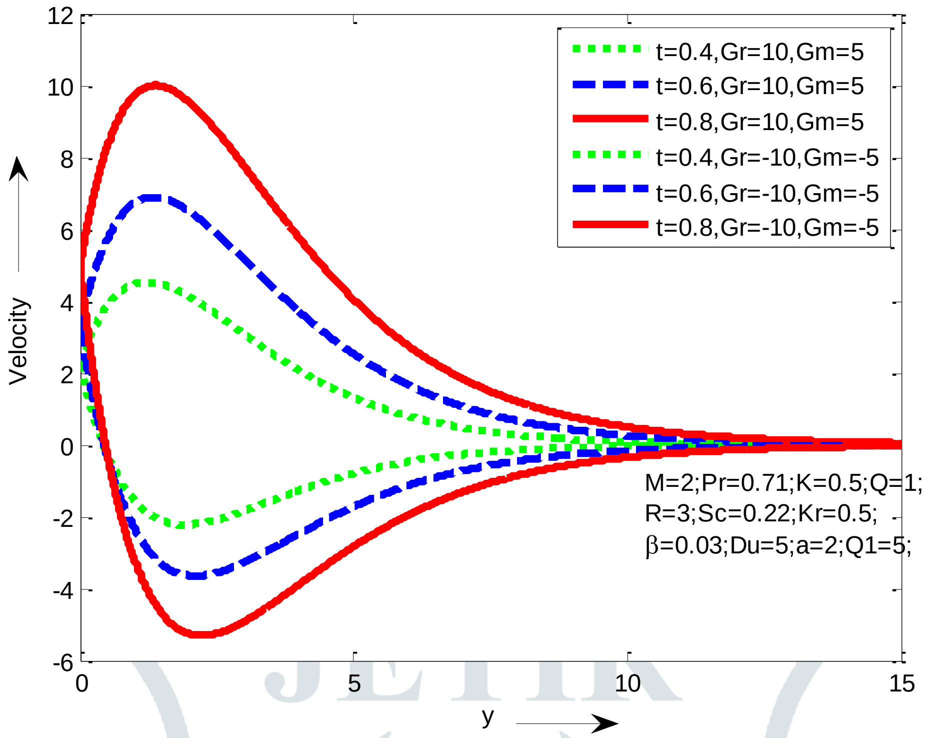

Figure 12. The influence of *t* on Velocity.

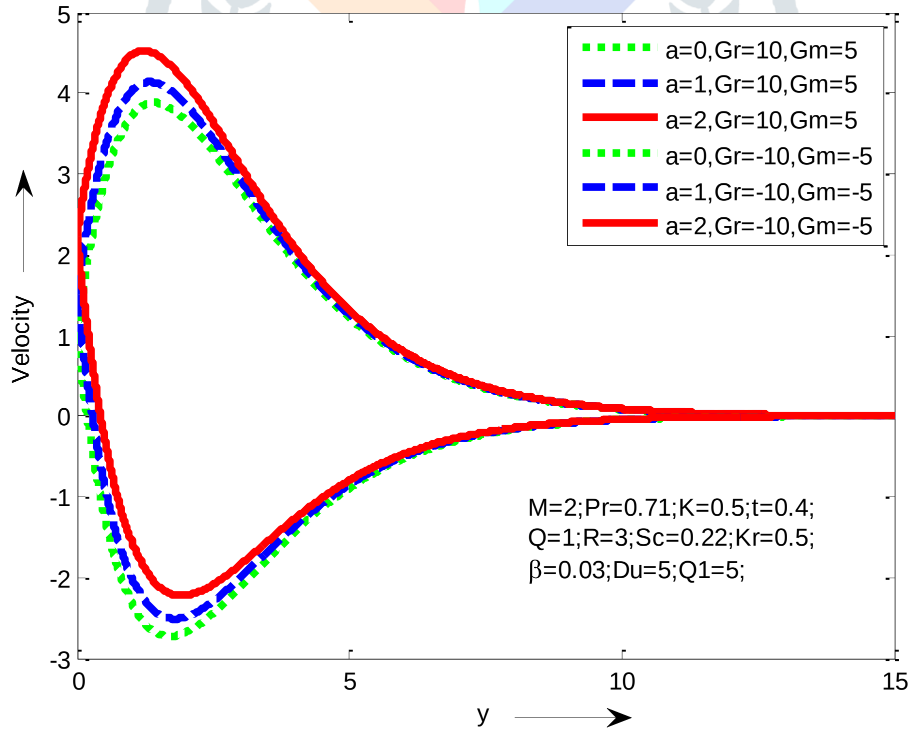

Figure 13. The influence of *'a'* on Velocity.

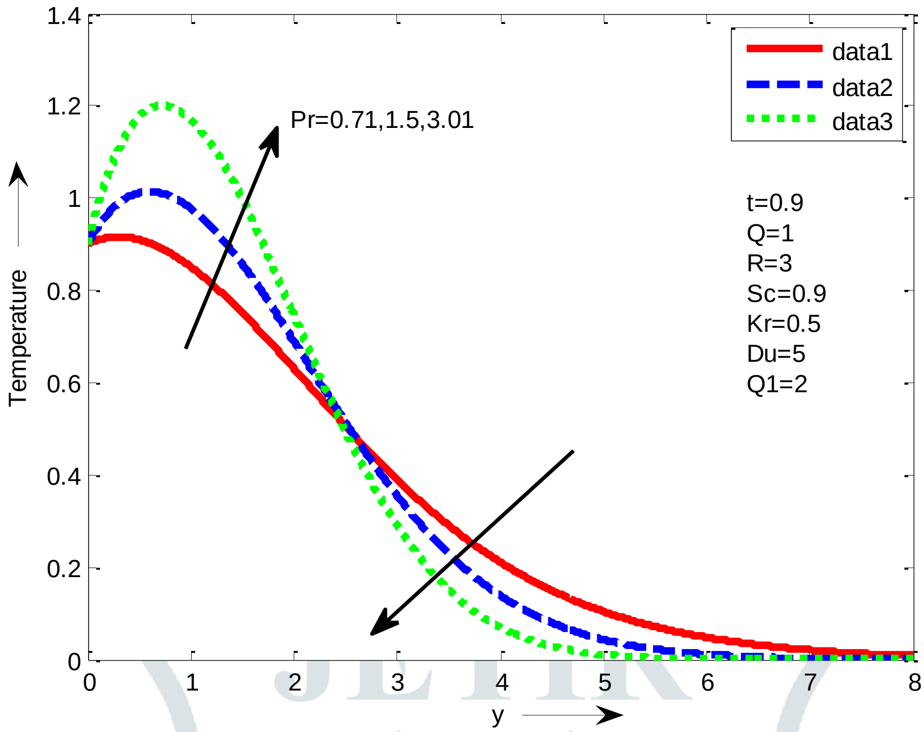

Figure 14. The influence of *Pr* on Temperature.

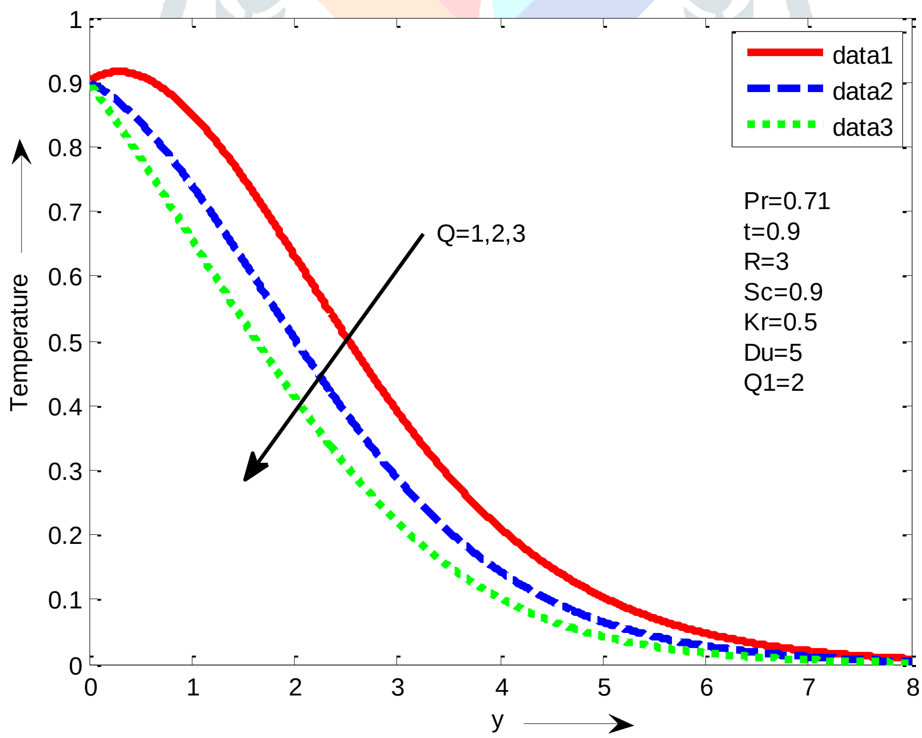

Figure 15. The influence of *Q* on Temperature.

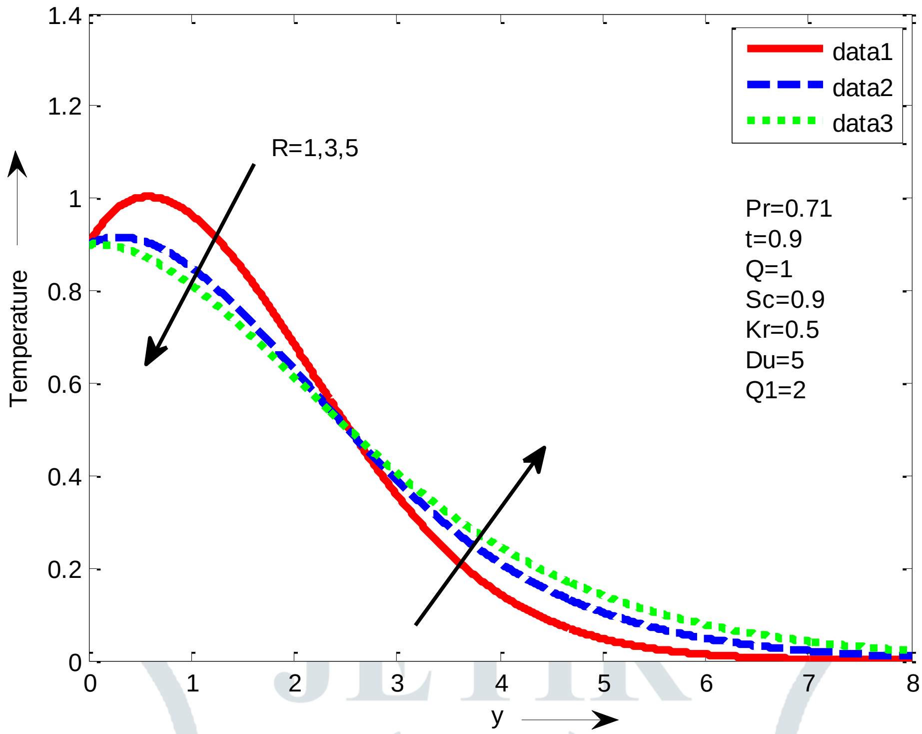

Figure 16. The influence of *R* on Temperature.

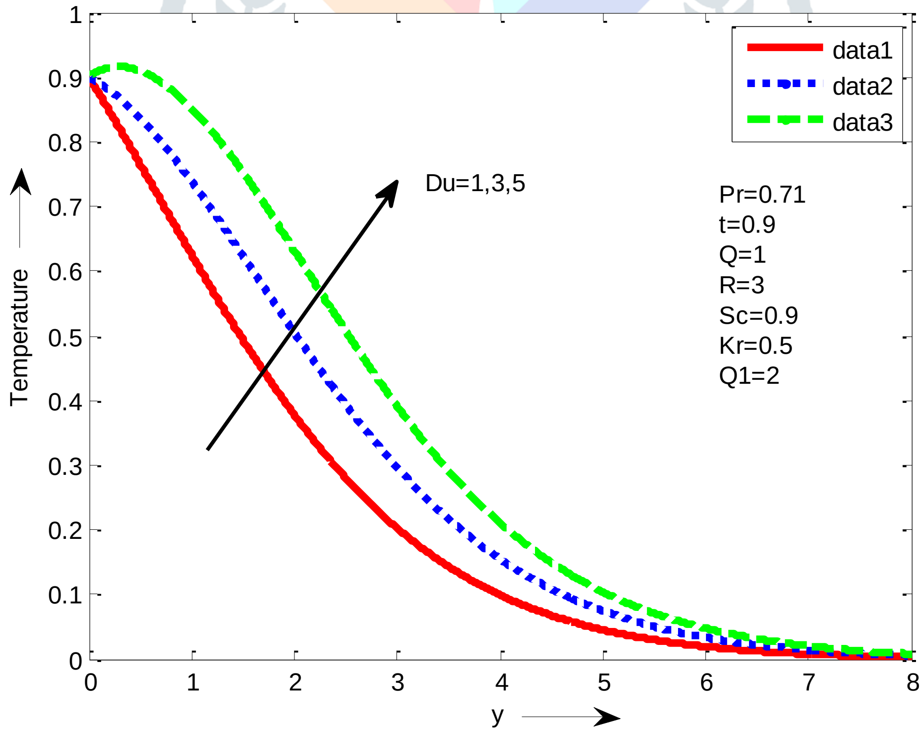

Figure 17. The influence of *Du* on Temperature.

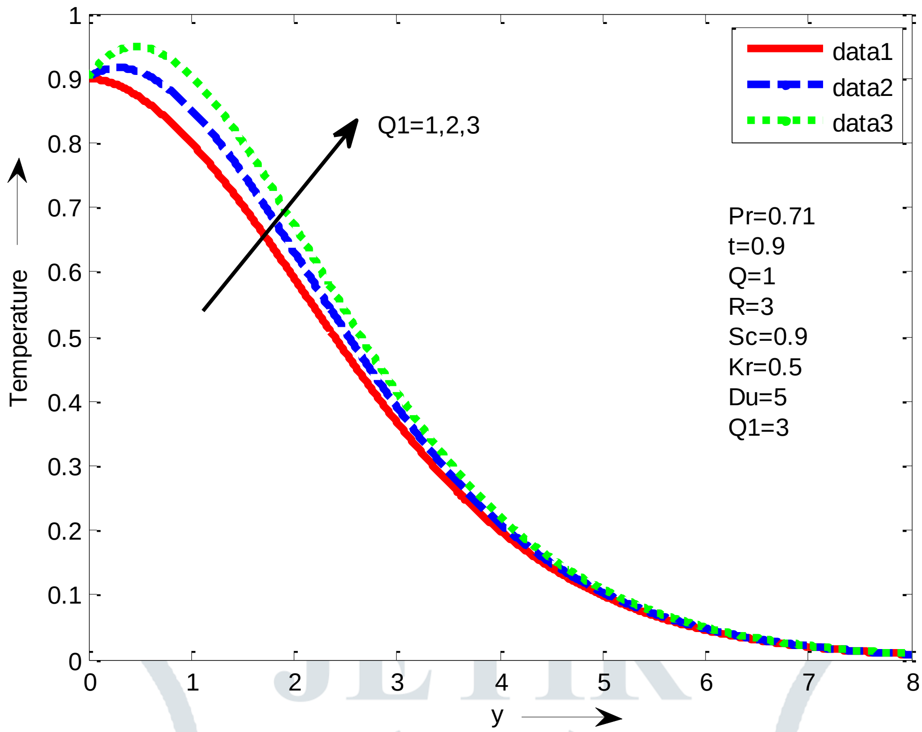

Figure 18. The influence of *Q1* on Temperature.

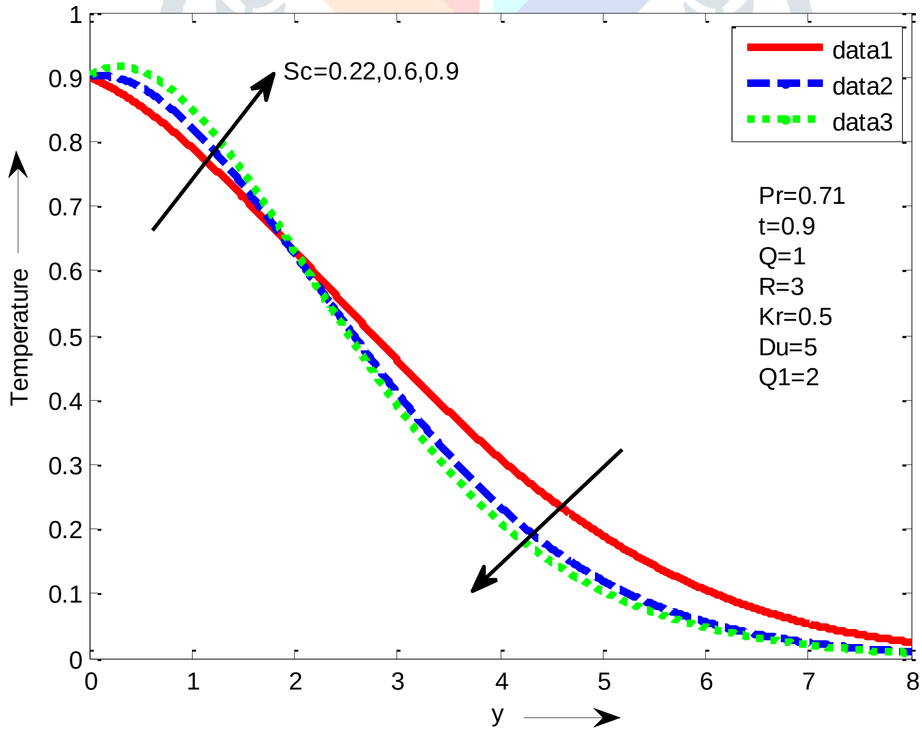

Figure 19. The influence of *Sc* on Temperature.

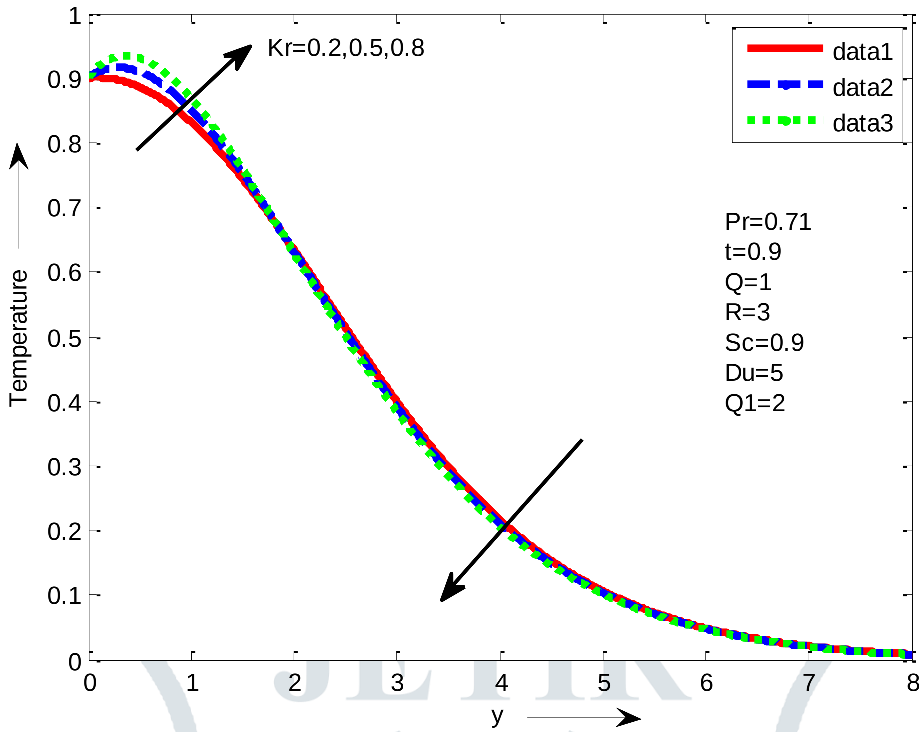

Figure 20. The influence of *Kr* on Temperature.

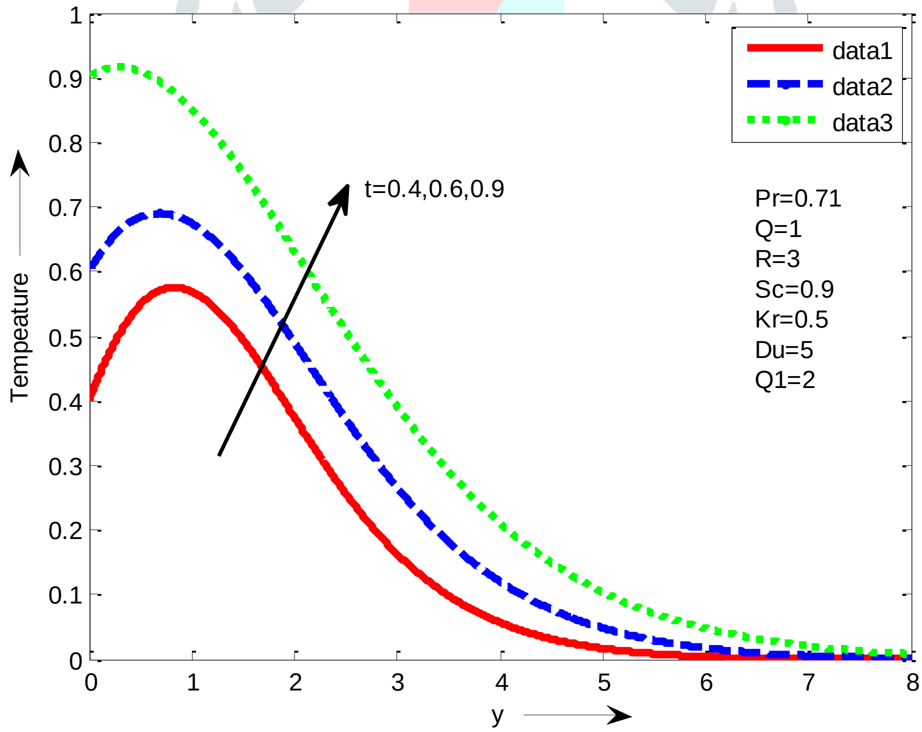

Figure 21. The influence of *t* on Temperature.

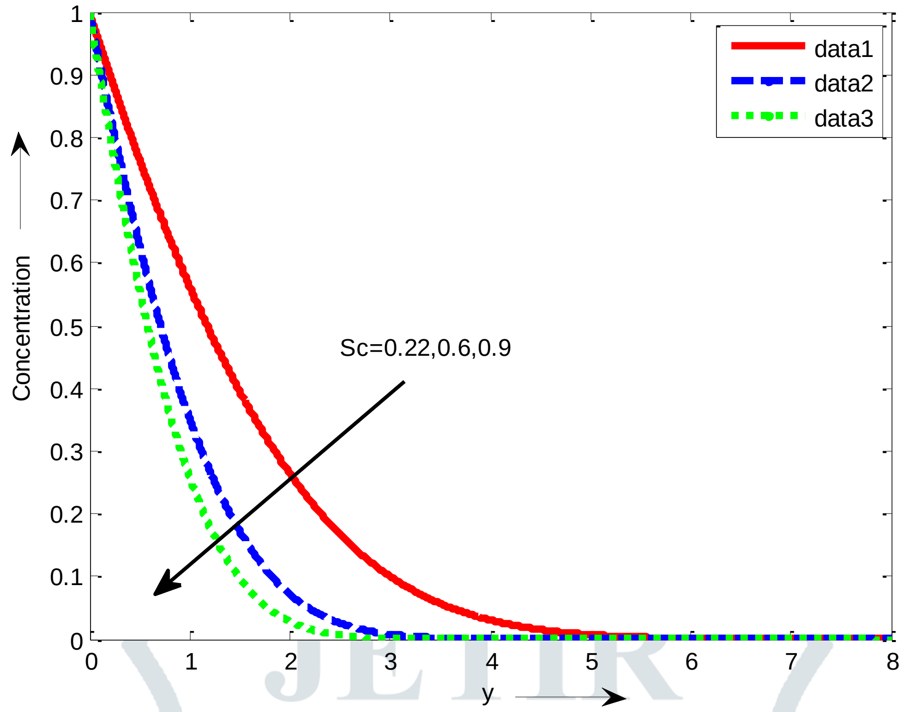

Figure 22. The influence of *Sc* on Concentration.

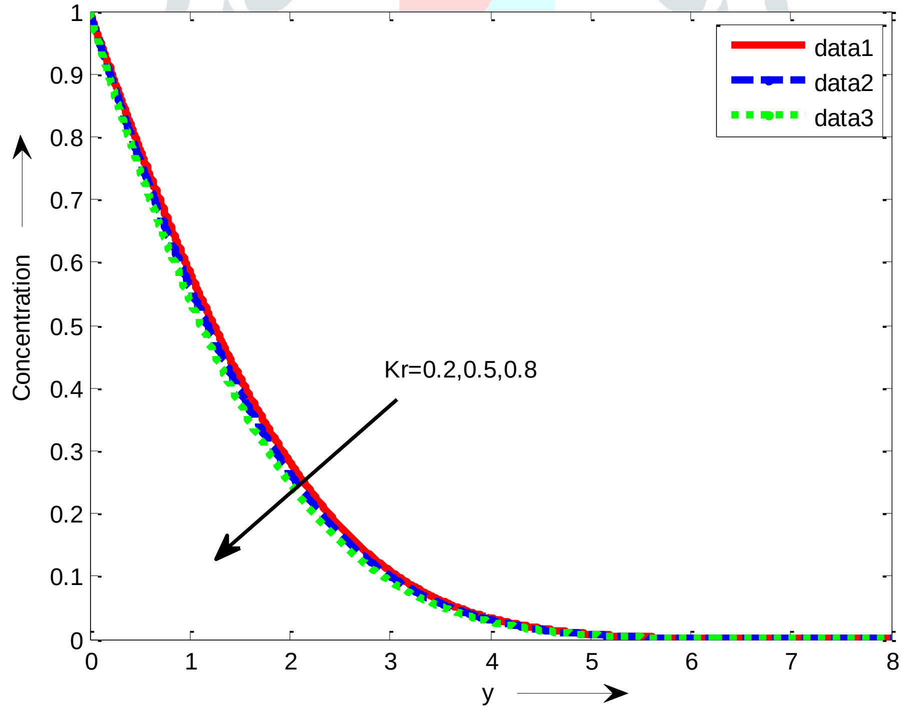

Figure 23. The influence of *Kr* on Concentration.

Table 1: Nusselt number

Pr	*R*	*Du*	*Q*	*Q1*	*t*	*Sc*	*Kr*	*Nu*
0.71	3	5	1	5	1	2	0.5	-0.5815

1.5	3	5	1	5	1	2	0.5	**-1.3613**
3.01	3	5	1	5	1	2	0.5	**-2.6870**
0.71	**4**	5	1	5	1	2	0.5	**-0.4347**
0.71	**5**	5	1	5	1	2	0.5	**-0.3363**
0.71	3	**6**	1	5	1	2	0.5	**-0.7314**
0.71	3	**8**	1	5	1	2	0.5	**-1.0311**
0.71	3	5	**2**	5	1	2	0.5	**-0.3609**
0.71	3	5	**3**	5	1	2	0.5	**-0.1803**
0.71	3	5	1	**6**	1	2	0.5	**-0.6720**
0.71	3	5	1	**8**	1	2	0.5	**-0.8529**
0.71	3	5	1	5	**0.6**	2	0.5	**-0.8027**
0.71	3	5	1	5	**0.8**	2	0.5	**-0.6819**
0.71	3	5	1	5	1	**3**	0.5	**-0.7342**
0.71	3	5	1	5	1	**4**	0.5	**-0.8788**
0.71	3	5	1	5	1	2	**0.3**	**-0.4861**
0.71	3	5	1	5	1	2	**0.4**	**-0.5344**

Table 2: Skin-friction coefficient: (for cooling *Gr>0,Gm>0*, for heating *Gr<0,Gm<0*)

M	*Pr*	*K*	*t*	*Q*	*R*	*Du*	*Sc*	*Kr*	*β*	*a*	*Q1*	*τ* (Gr=10, Gm=10)	*τ* (Gr=-10, Gm=-10)
7	**0.71**	**0.5**	**0.4**	**1**	**3**	**5**	**2**	**0.5**	**0.03**	**2**	**5**	**1.6442**	**0.8760**
8	0.71	0.5	0.4	1	3	5	2	0.5	0.03	2	5	**1.4618**	**1.1702**
9	0.71	0.5	0.4	1	3	5	2	0.5	0.03	2	5	**1.3965**	**1.3427**
7	**1.5**	0.5	0.4	1	3	5	2	0.5	0.03	2	5	**1.5122**	**1.0079**
7	**3.01**	0.5	0.4	1	3	5	2	0.5	0.03	2	5	**1.8204**	**0.6997**
7	0.71	**0.3**	0.4	1	3	5	2	0.5	0.03	2	5	**1.4320**	**1.2362**
7	0.71	**0.4**	0.4	1	3	5	2	0.5	0.03	2	5	**1.5302**	**1.0465**
7	0.71	0.5	**0.6**	1	3	5	2	0.5	0.03	2	5	**2.2065**	**1.5521**
7	0.71	0.5	**0.8**	1	3	5	2	0.5	0.03	2	5	**3.0497**	**2.5574**
7	0.71	0.5	0.4	**2**	3	5	2	0.5	0.03	2	5	**0.8256**	**1.6946**
7	0.71	0.5	0.4	**3**	3	5	2	0.5	0.03	2	5	**0.8896**	**1.6306**
7	0.71	0.5	0.4	1	**4**	5	2	0.5	0.03	2	5	**1.2778**	**1.2424**
7	0.71	0.5	0.4	1	**5**	5	2	0.5	0.03	2	5	**1.1660**	**1.3541**
7	0.71	0.5	0.4	**1**	3	**6**	2	0.5	0.03	2	5	**1.6168**	**0.9034**

7	0.71	0.5	0.4	**1**	3	**7**	2	0.5	0.03	2	5	**1.5894**	**0.9308**
7	0.71	0.5	0.4	1	3	5	**3**	0.5	0.03	2	5	**1.6525**	**0.8677**
7	0.71	0.5	0.4	1	3	5	**4**	0.5	0.03	2	5	**1.6566**	**0.8635**
7	0.71	0.5	0.4	1	3	5	2	**0.3**	0.03	2	5	**1.5322**	**0.9880**
7	0.71	0.5	0.4	1	3	5	2	**0.4**	0.03	2	5	**1.5903**	**0.9298**
7	0.71	0.5	0.4	1	3	5	2	0.5	**0.04**	2	5	**1.3757**	**1.5204**
7	0.71	0.5	0.4	1	3	5	2	0.5	**0.05**	2	5	**1.3669**	**1.8555**
7	0.71	0.5	0.4	1	3	5	2	0.5	0.03	**3**	5	**2.3473**	**1.5791**
7	0.71	0.5	0.4	1	3	5	2	0.5	0.03	**4**	5	**3.4322**	**2.6640**
7	0.71	0.5	0.4	1	3	5	2	0.5	0.03	2	**6**	**1.6482**	**0.8720**
7	0.71	0.5	0.4	1	3	5	2	0.5	0.03	2	**7**	**1.6521**	**0.8680**

The bold values in table indicate the variation of the parameters and variables present in the corresponding Columns

Table 3: Sherwood number

Sc	*Kr*	*Sh*
2	0.5	**1.1666**
3	0.5	**1.4288**
4	0.5	**1.6499**
2	**0.3**	**1.4509**
2	**0.4**	**1.5519**

Effects of Casson parameter *(β)*, acceleration parameter *(a)*, Schmidt number *(Sc)*, magnetic parameter *(M)*, thermal Grashof number *(Gr)*, mass Grashof number *(Gm)*, permibility parameter *(K)*, Radiation parameter *(R)*, chemical reaction parameter *(Kr)*, Dufour number *(Du)*, Radiation absorption *(Q1)*, heat absorption parameter *(Q)*, Prandtl number *(Pr)* and time *(t)* on Skin friction coefficients, Nusselt number and Sherwood number is presented in tables. **From table (1),** the effects of Nusselt number increases with the values *R, Q and t* increases and reduces when *Pr, Du, Q1, Sc and Kr* increases. **From table (2),** the effects of Skin friction coefficients in case of cooling and heating. From this it is clear that Skin friction coefficients increases with the values of *Pr, K, t, Q, Sc, Kr and Q1* increases and it decreases with the values of *M, R, Du, β, a and t* increases in case of cooling. But it is opposite phenomenon in case of heating

From table (3), the influence of Sherwood number coefficients increases with the values of *Sc, Kr or t* increases.

Conclusion:

From the above work the following conclusions are made:

- Velocity decreases with *M, Pr, K, Q, R, Sc, Kr or Q1* increases in case of cooling and reverse phenomenon is observed in case of heating. Velocity increases with *Gr, Gm, Du, β, t or a* increases in case of cooling and it is noticed opposite behavior in case of heating. But both the cases velocity increases with time (t) increases.

- Temperature increases with the values of *Du Q1 or t* increases and reduces when the value of *Q* increases. Temperature increases initially and slowly reduces with the values of *Pr, Sc or Kr* increases and reverse effect when the value of *R* increases.
- The concentration decreases as *Kr or Sc* increases.
- Nusselt number increases with the values of *R, Q or t* increases and it decay when *Pr, Du, Q1, Sc and Kr* increases.
- Sherwood number increases as *Kr, Sc or t* increases.
- Skin friction coefficients increases with the values of *Pr, K, t, Q, Sc, Kr or Q1* increases and it decreases as *M, R, Du, a or β* increases in case of cooling. But the reverse effect is noticed in case of heating. But both the case Skin friction coefficients increases with time (t) increases.

References:

[1] Casson, N., (1959), A flow equation for pigment-oil suspensions of the printing ink type. Rheology of disperse systems.

[2] McGregor, J.L., (1970). The application of the minimal energy hypothesis to a casson fluid. The bulletin of mathematical biophysics, 32(2), pp.249-262.

[3] Mernone, A.V., Mazumdar, J.N. and Lucas, S.K., (2002). A mathematical study of peristaltic transport of a Casson fluid. Mathematical and Computer Modelling, 35(7-8), pp.895-912.

[4] Raptis, A. and Perdikis, C., (2004). Unsteady flow through a highly porous medium in the presence of radiation. Transport in Porous Media, 57(2), pp.171-179.

[5] Boyd, J., Buick, J.M. and Green, S., (2007). Analysis of the Casson and Carreau-Yasuda non-Newtonian blood models in steady and oscillatory flows using the lattice Boltzmann method. Physics of Fluids, 19(9), p.093103.

[6] Mustafa, M., Hayat, T., Pop, I. and Aziz, A., (2011). Unsteady boundary layer flow of a Casson fluid due to an impulsively started moving flat plate. Heat Transfer—Asian Research, 40(6), pp.563-576.

[7] Raptis, A., (2011). Free convective oscillatory flow and mass transfer past a porous plate in the presence of radiation for an optically thin fluid. Thermal Science, 15(3), pp.849-857.

[8] Hayat, T., Shehzad, S.A. and Alsaedi, A., (2012). Soret and Dufour effects on magnetohydrodynamic (MHD) flow of Casson fluid. Applied mathematics and Mechanics, 33(10), pp.1301-1312.

[9] Nadeem, S., Haq, R.U. and Lee, C., (2012). MHD flow of a Casson fluid over an exponentially shrinking sheet. Scientia Iranica, 19(6), pp.1550-1553.

[10] Shehzad, S.A., Hayat, T., Qasim, M. and Asghar, S., (2013). Effects of mass transfer on MHD flow of Casson fluid with chemical reaction and suction. Brazilian Journal of Chemical Engineering, 30(1), pp.187-195.

[11] Bhattacharyya, K., (2013). Boundary layer stagnation-point flow of casson fluid and heat transfer towards a shrinking/stretching sheet. Frontiers in Heat and Mass Transfer (FHMT), 4(2).

[12] Bhattacharyya, K., (2013). MHD stagnation-point flow of Casson fluid and heat transfer over a stretching sheet with thermal radiation. Journal of Thermodynamics, 2013.

[13] Mukhopadhyay, S. and Vajravelu, K., (2013). Diffusion of chemically reactive species in Casson fluid flow over an unsteady permeable stretching surface. Journal of Hydrodynamics, 25(4), pp.591-598.

[14] Subba Rao, A., Ramachandra Prasad, V., Bhaskar Reddy, N. and Anwar Bég, O., (2015). Heat Transfer in a Casson Rheological Fluid from a Semi-infinite Vertical Plate with Partial Slip. Heat Transfer—Asian Research, 44(3), pp.272-291.

[15] Mukhopadhyay, S., De, P.R., Bhattacharyya, K. and Layek, G.C., (2013). Casson fluid flow over an unsteady stretching surface. Ain Shams Engineering Journal, 4(4), pp.933-938.

[16] Shehzad, S.A., Hayat, T., Qasim, M. and Asghar, S., (2013). Effects of mass transfer on MHD flow of Casson fluid with chemical reaction and suction. Brazilian Journal of Chemical Engineering, 30(1), pp.187-195.

[17] Sarojamma, G., Vasundhara, B. and Vendabai, K., (2014). MHD Casson fluid flow, heat and mass transfer in a vertical channel with stretching Walls. Int. J. Sci and Innovative Mathhematical Res, 2(10), pp.800-810.

[18] Pramanik, S., (2014). Casson fluid flow and heat transfer past an exponentially porous stretching surface in presence of thermal radiation. Ain Shams Engineering Journal, 5(1), pp.205-212.

[19] Animasaun, I.L., (2015). Effects of thermophoresis, variable viscosity and thermal conductivity on free convective heat and mass transfer of non-darcian MHD dissipative Casson fluid flow with suction and nth order of chemical reaction. Journal of the Nigerian Mathematical Society, 34(1), pp.11-31.

[20] Hussanan, A., Salleh, M.Z., Tahar, R.M. and Khan, I., (2014). Unsteady boundary layer flow and heat transfer of a Casson fluid past an oscillating vertical plate with Newtonian heating. PloS one, 9(10), p.e108763.

[21] Makanda, G., Shaw, S. and Sibanda, P., (2015). Diffusion of chemically reactive species in Casson fluid flow over an unsteady stretching surface in porous medium in the presence of a magnetic field. Mathematical problems in engineering, 2015.

[22] Sharada, K. and Shankar, B., (2015). MHD mixed convection flow of a Casson fluid over an exponentially stretching surface with the effects of soret, dufour, thermal radiation and chemical reaction. World Journal of Mechanics, 5(09), p.

[23] Saqib, M., Ali, F., Khan, I. and Sheikh, N.A., (2018). Heat and mass transfer phenomena in the flow of Casson fluid over an infinite oscillating plate in the presence of first-order chemical reaction and slip effect. Neural Computing and Applications, 30(7), pp.2159-2172.

[24] Reddy, M.G., (2015). Unsteady radiative-convective boundary-layer flow of a Casson fluid with variable thermal conductivity. Journal of Engineering Physics and Thermophysics, 88(1), pp.240-251.

[25] Kirubhashankar, C.K., Ganesh, S. and Ismail, A.M., (2015). Casson fluid flow and heat transfer over an unsteady porous stretching surface. Applied Mathematical Sciences, 9(7), pp.345-351.

[26] Ahmed, N., Khan, U., Khan, S.I., Bano, S. and Mohyud-Din, S.T., (2017). Effects on magnetic field in squeezing flow of a Casson fluid between parallel plates. Journal of King Saud University-Science, 29(1), pp.119-125.

[27] Kumar, P.S. and Gangadhar, K., (2015). Effect of chemical reaction on slip flow of MHD Casson fluid over a stretching sheet with heat and mass transfer. Adv. Appl. Sci. Res, 6(8), pp.205-223.

[28] Das, M., Mahato, R. and Nandkeolyar, R., (2015). Newtonian heating effect on unsteady hydromagnetic Casson fluid flow past a flat plate with heat and mass transfer. Alexandria Engineering Journal, 54(4), pp.871-879.

[29] Gireesha, B.J., Mahanthesh, B. and Rashidi, M.M., (2015). MHD boundary layer heat and mass transfer of a chemically reacting Casson fluid over a permeable stretching surface with non-uniform heat source/sink. Int. J. Ind. Math, 7(3), pp.247-260.

[30] Sarma, D. and Pandit, K.K., (2016). Effects of hall current, rotation and Soret effects on MHD free convection heat and mass transfer flow past an accelerated vertical plate through a porous medium. Ain Shams Engineering Journal.

[31] Raju, C.S.K., Sandeep, N., Sugunamma, V., Babu, M.J. and Reddy, J.R.,(2016). Heat and mass transfer in magnetohydrodynamic Casson fluid over an exponentially permeable stretching surface. Engineering Science and Technology, an International Journal, 19(1), pp.45-52.

[32] Kataria, H.R. and Patel, H.R., (2016). Soret and heat generation effects on MHD Casson fluid flow past an oscillating vertical plate embedded through porous medium. Alexandria Engineering Journal, 55(3), pp.2125-2137.

[33] Khan, H., Qayyum, M., Khan, O. and Ali, M., (2016). Unsteady squeezing flow of Casson fluid with magnetohydrodynamic effect and passing through porous medium. Mathematical Problems in Engineering, 2016.

[34] Reddy, S.H., Rajua, M.C. and Reddyb, E.K., (2016). Radiation absorption and chemical reaction effects on MHD flow of heat generating Casson fluid past oscillating vertical porous plate. Frontiers in heat and mass Transfer, 7.

[35] Pushpalatha, K., Sugunamma, V., Reddy, J.R. and Sandeep, N., (2016). Heat and mass transfer in unsteady MHD Casson fluid flow with convective boundary conditions. International Journal of Advanced Science and Technology, 91, pp.19-38.

[36] Ullah, I., Bhattacharyya, K., Shafie, S. and Khan, I., (2016). Unsteady MHD mixed convection slip flow of Casson fluid over nonlinearly stretching sheet embedded in a porous medium with chemical reaction, thermal radiation, heat generation/absorption and convective boundary conditions. PloS one, 11(10), p.e0165348.

[37] Mohan, S.R., Reddy, G.V., Varma, S.V.K. and Krishna, S.B., (2017). Thermal radiation and chemical reaction effects on unsteady MHD free convection flow of a viscous dissipative Casson fluid past an exponentially infinite vertical plate through porous medium with TGHS. i-Manager's Journal on Mathematics, 6(2), p.17.

[38] Veeresh, C., Varma, S.V.K., Kumar, A.G.V., Umamaheswar, M. and Raju, M.C., (2017). Joule heating and thermal diffusion effects on MHD radiative and convective Casson fluid flow past an oscillating semi-infinite vertical porous plate. Frontiers in Heat and Mass Transfer, 8(1).